ASIAN JOURNAL OF CIVIL ENGINEERING (BHRC) VOL. 18, NO. 2(2017)
PAGES 285-309

PREDICTION OF PUNCHING SHEAR CAPACITY OF RC FLAT SLABS USING ARTIFICIAL NEURAL NETWORK

N. A. Safiee[*1] and A. Ashour[2]
[1]Department of Civil Engineering, University Putra Malaysia, 43400 Serdang, Selangor
[2]School of Engineering, University of Bradford, BD7 1DP, UK

Received: 14 June 2016; **Accepted:** 29 August 2016

ABSTRACT

Punching shear of flat slabs is a local, brittle failure that may occur before the more favourable ductile flexural failure. This study develops an artificial neural network (ANN) modelling for the prediction of punching shear strength of flat slabs using 281 test data available in the literature. The paper also evaluates the current design codes for the prediction of punching shear capacity of reinforced concrete flat slabs using the test results reported in the literature. Furthermore, a parametric study was conducted using the trained ANN to establish the trend of the main influencing variables on the punching shear capacity of flat slabs. The results were, then, employed to develop a simplified equation for the prediction of the characteristic/design punching shear strength of flat slabs based on the design assisted by testing approach proposed in Annex D of EN 1990.

Keywords: Punching shear; flat slabs; slab-column connections; neural network.

1. INTRODUCTION

The structural concepts of buildings often comprise concrete flat slabs locally supported by columns without beams. One advantage of flat slabs is the easier construction compared with ribbed or mushroom slabs. It also permits greater flexibility in the disposition of rooms that are simply enclosed by easily removable non-structural walls. Without beams, flat slabs provide more headroom or permit more storeys to be accommodated within the same building height than other types of slab systems. The disadvantage, however, is the combination of locally high negative bending moments and shear forces around columns, which increases the sensitivity of this zone to brittle punching shear failure. In this failure mode, the slab suddenly collapses around a truncated cone above the column, followed by a drop in the load-bearing capacity of the slab, which may eventually lead to a progressive

[*]E-mail address of the corresponding author: norazizi@upm.edu.my (N. A. Safiee)

Archive of SID

www.SID.ir

collapse of the entire structure. The design of flat slabs is generally governed by serviceability limits on deflection or by ultimate punching shear strength of slab-column connections. Nowadays, there are few options to predict the behaviour and strength of punching shear of flat slabs using developed techniques such as finite element analysis and artificial neural network modelling [1, 2]. Furthermore, few design guidelines have been developed for calculating the punching shear capacity of flat slabs such as BS8110-97 [3], CEB-FIP-90 [4], Euro-code 2 [5], ACI 318-11 [6] and CSA-A23.03-04 [7]. However, the equations proposed by these codes are empirical, practically governed by a statistical regression against limited test results available at the time of derivation. Moreover, they adopt considerably different parameters as well as their limitations, leading to discrepancy of punching shear strength among various code predictions.

The previous studies [1, 8, 9 & 10] focused on investigating the main factors influencing the punching shear capacity of flat slabs. Among others, the concrete compressive strength is the most influential parameter on punching shear development [8, 11, 12, 13 & 14]. The shear strength increases with the increase of concrete compressive strength but it is not linearly proportional relationship. Moe [12] reported that the shear strength of slab-column connections is primarily controlled by the tensile-splitting strength, which is assumed to be proportional to $\sqrt{f_c'}$, where f_c' is the concrete compressive strength. Other important parameter is the slab effective depth, d. As d increases, the shear strength decreases; that is known as the size effect. The size effect is considered in BS8110-97 and CEB-FIP-90 but not in ACI 318-11 and CSA-A23.03-04. The ratio of flexural reinforcement,ρ, is also one of the significant factors on punching shear strength. The punching shear strength of flat slabs is expected to increase with the increase of flexural reinforcement ratio. Higher reinforcement ratios, however, lead to a more brittle structural behaviour. The percentage of flexural reinforcement is often used as an index for the dowel effect, which could carry about 30% of the total shear capacity [15 & 16]. However, Vintzeleou and Tassios [17] indicated that possible failure model of dowel mechanism is governed by splitting of concrete and not punching shear.

This paper develops an artificial neural network for the prediction of punching shear capacity of flat slabs. It also assesses four design codes for the prediction of punching shear capacity of reinforced concrete flat slabs against 281 test results available in the literature. Furthermore, it presents a simplified equation for the prediction of the design punching shear strength of flat slabs based on the design assisted by testing approach proposed in Annex D of EN 1990 [18].

2. ASSESSMENT OF EXISTING CODE EQUATIONS FOR PUNCHING SHEAR OF FLAT SLABS

Many available design codes can be used in determining the punching shear strength of flat slabs. This section of the paper evaluates and compares shear strength formulas in existing codes of practice. Table 1 gives various expressions proposed by codes for shear strength calculation and the location of the critical punching shear failure plane. For convenience, the same symbols are used for all design guidelines but they may be different from the original

Archive of SID

www.SID.ir

guideline document. Furthermore, the steel and concrete material safety factors are assigned to 1.0 in all codes. The CEB-FIP-90 and EC2 design guidelines are very similar as indicated in Table 1 and, therefore, CEB-FIP-90 will be only considered in further analysis. ACI 318-11 is also similar to CSA-A23.03-04 but the calibration coefficient is slightly different.

Table 1: Shear strength equations and critical shear failure planes in different design codes

Codes	Equations	Limitations on parameters	Critical shear failure plane
ACI 318-11	$v_c = 0.33\lambda\sqrt{f_c'}$	-	$0.5d$
CSA-A23.03-04	$v_c = 0.38\lambda\sqrt{f_c'}$	$\sqrt{f_c'} \leq 8MPa$	$0.5d$
CEB-FIP-90 Eurocode 2	$v_c = C_{Rd,c}k(100\rho f_c')^{1/3}$	$k = 1 + \sqrt{\frac{200}{d}} \leq 2.0$, $\rho \leq 0.02$	$2.0d$
BS8110-97	$v_c = 0.79(100\rho)^{0.33}k^{0.25}\left(\frac{f_{cu}}{25}\right)^{0.33}$	$k = \frac{400}{d} \geq 1.0$, $\rho \leq 0.03$, $f_{cu} \leq 40MPa$	$1.5d$

Note: f_c' is the cylinder compressive strength (N/mm^2), f_{cu} is the cube compressive strength in (N/mm^2), λ is the density modification factor (λ = 1.0 for normal weight concrete, 0.85 for sand-lightweight concrete and 0.75 for all lightweight concrete), $C_{Rd,c}$ the a calibration factor ($C_{Rd,c} = 0.18$ in EC2 and $C_{Rd,c} = 0.12$ in CEB-FIP-90), d is the slab effective depth (mm), k is the size effect parameter and ρ is the ratio of flexure reinforcement.

Different design codes adopt considerably different parameters in their equations as well as their limitations but the only same parameter in all equations is the concrete compressive strength. However, it is raised to different powers: 0.5 in ACI 318-11 and CSA-A23.03-04, whereas 0.33 in CEB-FIP-90 and BS8110-97. Both the effective depth and flexure reinforcement ratio are considered by BS8110-97 and CEB-FIP-90 but neither is included in ACI 318-11 and CSA-A23.03-04 code equations. This may lead to discrepancy of prediction of punching shear strength among various code predictions. Furthermore, various codes impose different limits on influencing parameters as stated in Table 1, indicating that they were calibrated on a limited range of test results.

The critical perimeter also becomes a main concern in calculating the punching shear strength where current codes recommend different critical perimeter measured from the loaded column face, for example ACI 318-11 and CSA-A23.03-04 use a perimeter at $0.5d$ measured from the loaded face, while, in BS8110-97 and CEB-FIP-90, the perimeter of the punching area is taken at $1.5d$ and $2.0d$, respectively, from the face of the loaded area.

The variations of punching shear strength calculated by each code against the three influencing parameters are presented in Fig. 1 for compressive strength, f_c', Fig. 2 for slab effective depth, d, and Fig. 3 for flexural reinforcement ratio, ρ. Fig. 1 indicates that the punching shear strengths predicted by various codes against the compressive strength are

Archive of SID

www.SID.ir

different. In Fig. 1, the calculated punching shear strength is calculated for $d = 150mm$ and ρ = 1.2%, while compressive strength varies. The highest calculated punching shear is produced by CSA-A23.03-04 code, followed by ACI 318-11 code with very similar trend (for up to $f_c^{'}$ = 64 MPa). On the other hand, the punching shear strength trends obtained by BS8110-97 and CEB-FIP-90 show a different pattern with much smaller magnitude than CSA-A23.03-04 and ACI 318-11. Since a limiting value for f_{cu} was imposed by BS8110-97 code, the predicted shear strength was constant for f_{cu} > 40MPa ($f_c^{'}$ = 32 MPa). This large gap among codes (more than 300% in case of $f_c^{'}$ > 50 MPa) may be attributed to the influence of other parameters, such as flexural reinforcement and effective depth that are ignored by ACI318-11 and CSA-A23.03-04.

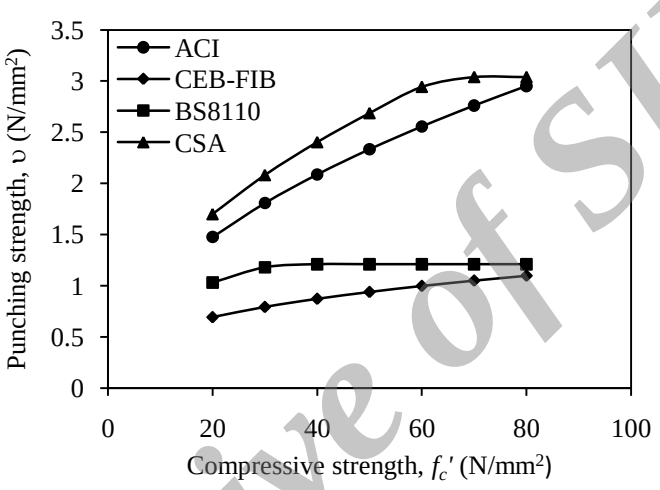

Figure 1. Variation of punching shear strength υ against the compressive strength, $f_c^{'}$

Fig. 2 shows the variation of punching shear strength predicted by the four codes against the effective depth, d. To rationalize the calculation of punching shear strength, $f_c^{'}$ and ρ are kept constant at 35 N/mm^2 and 1.2%, respectively, while d is increased accordingly throughout the simulation. As an effect of not taking into account the effective depth, d, in their calculation, ACI318-11 and CSA-A23.03-04 produced constant results for punching shear strength throughout the variation of d. However, the punching shear strengths by BS8110-97 and CEB-FIB-90 reduces as d increases. Fig. 2 also indicates that the punching shear strength prediction of ACI318-11 and CSA-A23.03-04 could be twice as high as that predicted by BS8110-97 and CEB-FIP-90.

The effect of flexural reinforcement ratio, ρ on the punching shear strength predicted by all four codes is shown in Fig. 3. In this calculation, $f_c^{'}$ and d are kept constant at 35 N/mm^2 and 150mm, respectively, while ρ is increased accordingly throughout the analysis. The calculated punching shear strength resulted in constant values for ACI 318-11 and CSA-A23.03-04 equations for various flexural reinforcements as their equations are independent on ρ, whereas the shear strength obtained by BS8110-97 and CEB-FIB-90 increases with the increase of ρ. The largest shear strength is produced by CSA-A23.03-04 code while the smallest is produced by CEB-FIB-90.

Archive of SID

www.SID.ir

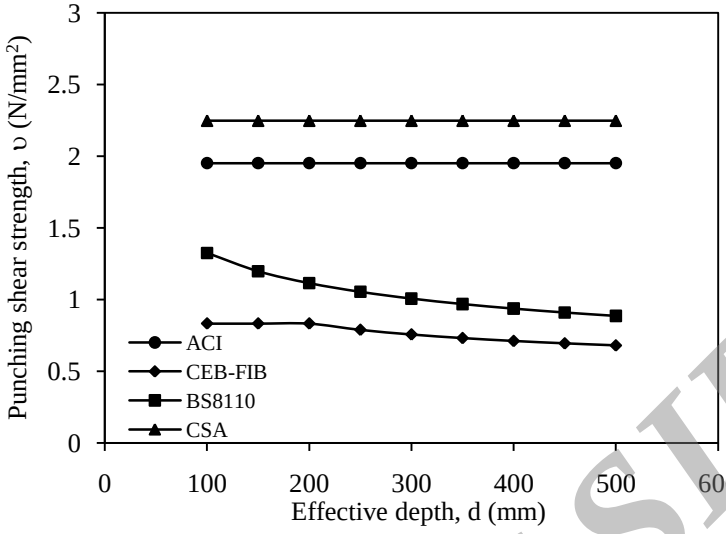

Figure 2. Variation of punching shear strength υ against the effective depth, d

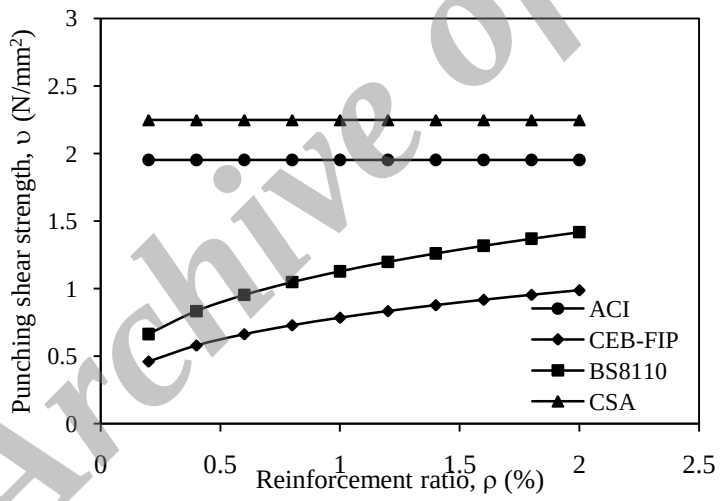

Figure 3. Variation of punching shear strength υ against the flexural reinforcement ratio, ρ.

Overall, it was observed that the shear strengths predicted by CSA-A23.03-04 and ACI 318-11 codes are generally larger than that obtained from BS8110-97 and CEB-FIP-90. However, as the critical perimeter in the BS8110-97 and CEB-FIP-90 ($1.5d$ and $2.0d$, respectively) is larger than that in CSA-A23.03-04 and ACI 318-11 codes ($0.5d$ in both codes), the punching shear capacities obtained from all codes are expected to get closer to each other.

Archive of SID

www.SID.ir

3. EXPERIMENTAL DATABASE

A total of 281 experimental data of reinforced concrete flat slabs tested under symmetrical punching shear were collected from the related literature [8,12,14,19-45]. The details of test specimens including their sources are presented in Appendix A. The database is initially used for assessing the four design code equations presented in Table 1 by comparing their predictions against the experimental punching shear capacities of flat slabs collected. The database is, then, employed to train and test the artificial neural network (ANN) for punching shear capacity prediction.

All specimens were reinforced concrete flat slab-column connections without drop panels, column capital or any type of shear reinforcement. The end conditions for all the selected test specimens were simply supported. The database included square and circular columns. The concrete compressive strength, $f_c^{'}$, for the collected specimens ranged between 12.3 and 119 MPa, the slab effective depth, d, from 35mm to 500mm, the ratio of flexure reinforcement, ρ, from 0.25% to 5.01% and the overall perimeter of loaded section, C, from 320 mm to 2080mm. The summary of statistical parameters for these variables is presented in Table 2 whereas Figs. 4 to 7 show the distribution of each parameter in the database.

Table 2: Statistical parameters of variables in the collected database

Parameters	Minimum	Maximum	Mean	Mode
Compressive strength, $f_c^{'}$ (MPa)	12.3	119	40.8	21-30
Slab effective depth, d (mm)	35	500	120	101-120
Flexure reinforcement ratio, ρ (%)	0.25	5.0%	1.19	0.6-1.0
Perimeter loaded section, C (mm)	320	2080	733.3	100-198

By observation, there is unbalance distribution of samples of each influencing parameters. In most cases, less number of specimens falls in higher values of each interval as shown in Figs. 4 to 7. Since this database will be used in neural network analysis as explained below, this may lead to a scatter and inaccuracy of neural network prediction for punching shear strength of flat slabs. Therefore, the specimens that fall in intervals with very less number of samples are excluded from the database for ANN modelling. Consequently, the total number of database is reduced to 241 for ANN modelling. However, all the 281 test specimens are used for the four code validations.

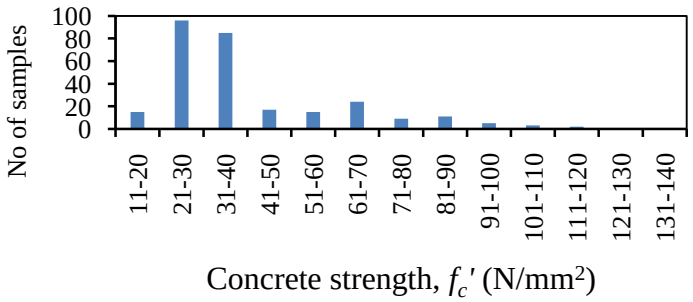

Figure 4. Distribution of concrete compressive strength in database

Archive of SID

www.SID.ir

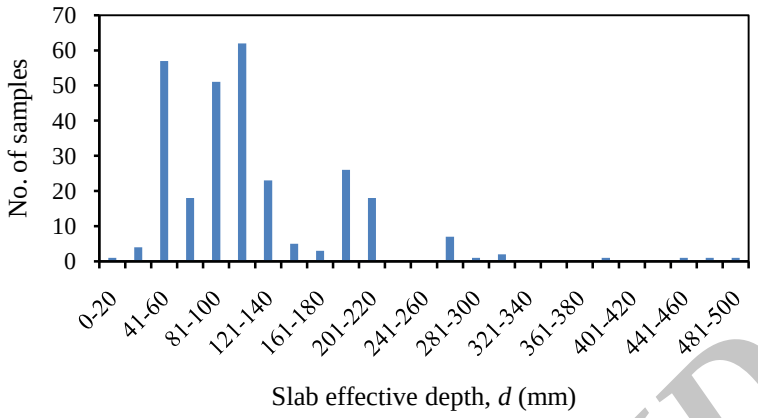

Figure 5. Distribution of the effective slab depth in database

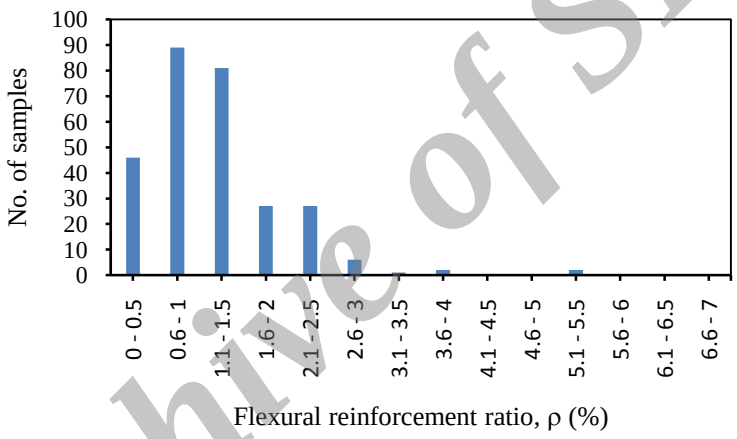

Figure 6. Distribution of flexural reinforcement ratio in database

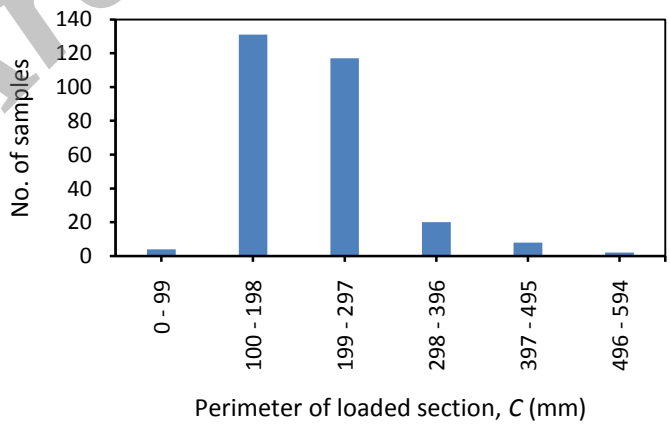

Figure 7. Distribution of perimeter of loaded section in database

Archive of SID

www.SID.ir

3.1 Comparisons between the available design codes and experiments

The ratio of the experimental to predicted punching shear capacities, V_{exp}/V_{pred}, evaluated by the four design codes for each test specimen in the database is presented in Appendix A, whereas the mean, standard deviation, coefficient of variation (COV%) and mean squared error (MSE%) of V_{exp}/V_{pred}, for all test specimens are presented in Table 3. The predicted punching shear capacities of the four codes are also plotted against the experimental values for all specimens in Figs. 8 to 11.

Table 3: Summary of statistical results for punching shear capacities predicted by available design codes

Design codes	Mean	Standard deviation	COV %	MSE %
ACI 318-11	1.28	0.376	29.359	21.92
BS 8110-97	1.21	0.255	21.13	10.86
CSA-A23.03-04	1.11	0.334	29.243	13.07
CEB-FIP-90	1.54	0.419	27.232	46.8

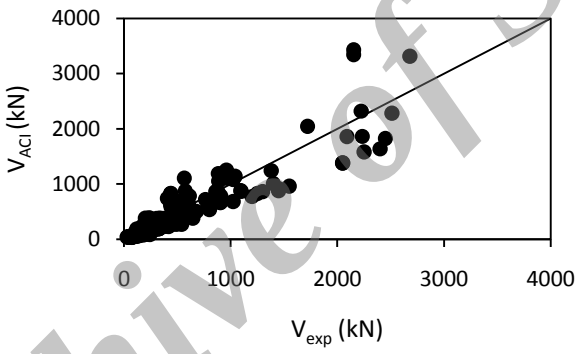

Figure 8 Predicted punching shear capacity, V_{pred} by ACI 318-11 vs experimental punching shear, V_{exp}

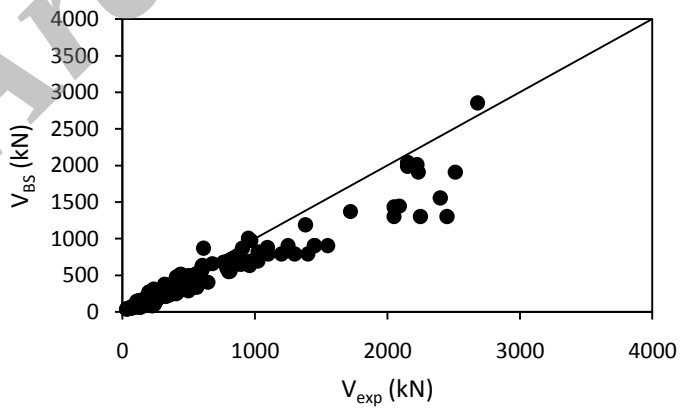

Figure 9. Predicted punching shear capacity, V_{pred} by BS8110-97 vs experimental punching shear, V_{exp}

Archive of SID

www.SID.ir

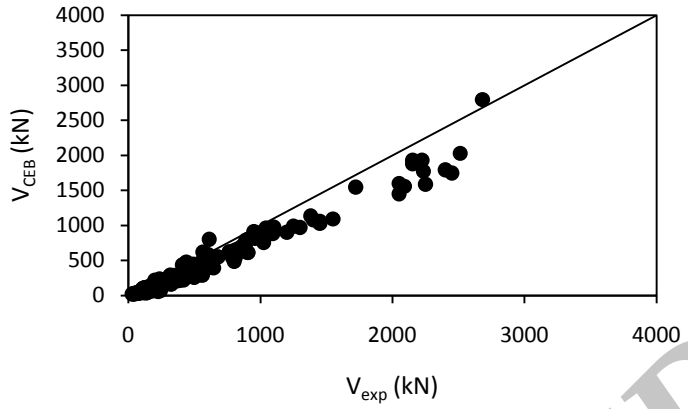

Figure 10. Predicted punching shear capacity, V_{pred} by CEB-FIP-90 vs experimental punching shear, V_{exp}

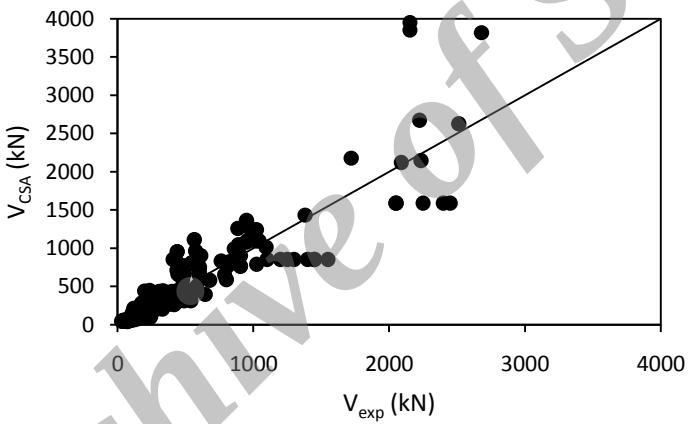

Figure 11. Predicted punching shear capacity, V_{pred} by CSA-A23.03-04 vs experimental punching shear, V_{exp}

The CEB-FIP-90 shows the most conservative and scatter results among other design codes as evidenced by the highest mean of 1.54 and standard deviation of 0.419. While BS 8110-97 prediction shows the least difference to the experimental values with the lowest MSE of 10.86%, a mean of 1.21 and least scatter with a standard deviation of 0.26.

4. ARTIFICIAL NEURAL NETWORK MODELLING

Artificial neural networks (ANN) are a class of computing devices that operate in a manner analogous to that of biological nervous systems. ANN is a powerful data driven, self-adaptive, flexible computational tool having the capability of capturing nonlinear and complex problems. ANNs can be used to solve a complex problem with no rational engineering solution, provided that there is a large number of experimental data available.

Archive of SID

www.SID.ir

Due to these reasons, ANNs have been chosen to predict the punching shear strength of reinforced concrete flat slabs. ANNs are configured from a number of parallel operating processors which are normally known as neurons connected through weighted links capable of solving complicated nonlinear problems [1, 2].

A multi layered feed-forward neural network consists of an input layer, one or more hidden layers and an output layer. The number of neurons in the input layer is equal to the number of parameters considered in the study. However, the number of hidden layers and the number of neurons in each hidden layer are chosen to minimise the error between the measured output and the network's output while maintaining the ability of the network to generalize [1, 2 & 46]. In designing the neural network models, a number of systematic procedures are followed such as data collection, pre-processing data, building the network, training and testing the model.

In this study, a feed-forward, back propagation neural network is used. The suitable architecture network was chosen after several trials performed on different architecture of hidden layers and neurons. A neural network with one input layer, one hidden layer and one output layer was eventually chosen to predict the punching shear capacity. A single hidden layer network was preferred due to its simpler architecture and better predictions especially for the testing dataset compared with ANNs having more neurons and also less likely to produce over fitting. Based on the experimental observation and established developed design equations from design codes, the parameters selected as the ANN inputs are compressive strength, f_c', slab effective depth, d, ratio of flexural reinforcement, ρ and overall perimeter of loaded section, C. The output is the punching shear capacity of flat slabs.

The total number of database used in ANN modelling is 241 after excluding the out-layers of input parameters as explained above. The input data was divided into three sets, namely training, validation and testing data sets. The first set consists of 70% of data and used to train the network. The validation and testing sets, each consisting of 15% of data, are used to validate and test the network generalization ability. The distribution of each influencing parameter across its range in the training subset was manually examined to ensure that it covers a good spread within the range considered.

Six different architectures of ANN have been tried and tested as listed in Table 4. For this study, only one hidden layer was tried to reduce the possibility of over fitting in case of a large number of hidden layers. The performance of each ANN architecture is evaluated by four statistical observations, namely mean, standard deviation, coefficient of variation (COV) and mean squared error (MSE) of V_{exp}/V_{pred} as listed in Table 4. Generally, the mean and standard deviation of V_{exp}/V_{pred} of punching shear capacity of flat slabs were similar among different ANN trials. However, among all trials, the 4 x 5 x 1 ANN presents the least error which was demonstrated by MSE of 2.56% and also less scatter with a standard deviation of 0.159. Furthermore, over-fitting problem rarely occurred in 4 x 5 x 1 ANN due to its simpler architecture and better predictions especially for the testing data set compared with ANNs having more neurons. Therefore, the 4 x 5 x 1 ANN was finally selected for further analysis – prediction for punching shear capacity for each data and parametric study. Fig. 12 compares the punching shear capacities obtained from the 4 x 5 x 1 ANN and experimental results as well as their corresponding linear regression. The ANN results show

Archive of SID

www.SID.ir

a good agreement with experimental results as evidenced by the coefficient of determination value, R^2, of 0.98 of the regression analysis as depicted in Fig. 12.

Table 4: Statistical results for 6 ANNs created

ANN architectures	Mean	Standard Deviation	COV (%)	MSE (%)
4 x 2 x 1	0.991	0.186	18.728	3.450
4 x 5 x 1	1.005	0.159	15.909	2.560
4 x 10 x 1	1.015	0.176	17.369	3.132
4 x 15 x 1	1.079	0.224	20.745	5.630
4 x 18 x 1	1.013	0.181	17.845	3.287
4 x 25 x 1	1.093	0.285	26.073	8.998

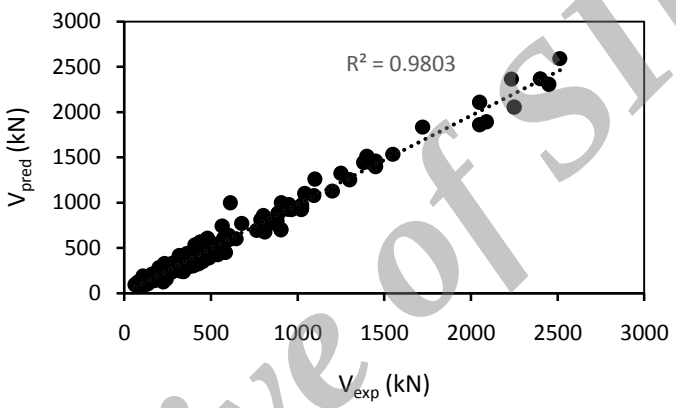

Figure 12. 4 x 5 x 1 network predicted vs experimental shear capacities

5. PARAMETRIC STUDY

The selected neural network model of 4 x 5 x 1 was used for a parametric study, where the effect of main input parameters were investigated on punching shear capacity of flat slabs. The values, at which various parameters were kept constant when one parameter was being changed in the analysis, are: d = 124 mm, f_c' = 43 MPa, ρ = 1.16% and C = 750 mm. These values are the mean values for the 241 specimens used in ANN modelling for each parameter.

5.1 Effect of slab effective depth

The influence of effective depth, d of flat slabs on punching shear strength is presented in Fig. 13. Due to the limited data available, this study has only focused on thin slabs with d ≤ 200mm. The ANN simulation indicates that the punching shear strength, is almost inversely proportional to the effective depth for $d < 100mm$. However, the punching shear strength predicted by ANN is almost unaffected for $200mm > d > 100mm$. For the case of $d < 100mm$, similar experimental results were also demonstrated by Regan [47] and Birkle and

Archive of SID

www.SID.ir

Dilger [48]. It also strongly agrees with the size effect parameter of BS8110-97 where the term $\sqrt[4]{1/d}$ is considered in calculating the punching shear strength. A similar term of size effect but with different power is also introduced by CEB-FIP-90. However, ACI 318-11 and CSA-A23.03-04 codes ignore the size effect in their punching shear strength equations even though many studies proved the significance of effective depth, *d* on the punching shear strength [9, 26, 33 & 47].

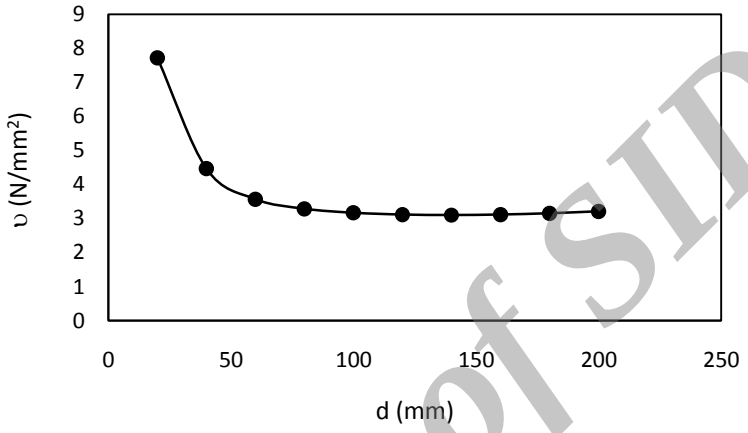

Figure 13. Slab effective depth, *d* effect on punching shear strength

5.2 Effect of concrete compressive strength

Fig. 14 shows the results of punching shear strength predicted by the 4 x 5 x 1 ANN when compressive strength, f_c' is increased. The punching shear strength of reinforced concrete flat slabs increases when concrete compressive strength increases as depicted in Fig. 14. However, the shear strength trend predicted by ANN is nonlinear as expressed in most codes. Theoretically, shear failure of concrete is mainly controlled by the concrete splitting tensile strength, that is generally assumed proportional to $\sqrt{f_c'}$ [12].

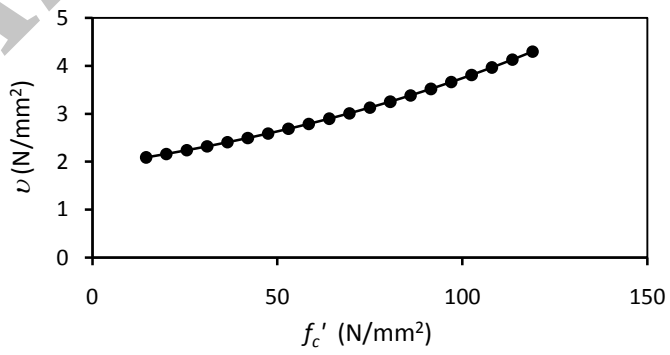

Figure 14 Concrete compressive strength, f_c', effect on punching shear strength

Archive of SID

www.SID.ir

5.3 Effect of Reinforcement ratio

Fig. 15 shows the effect of reinforcement ratio, ρ, on punching shear strength of reinforced concrete flat slabs. The punching shear strength of flat slabs increases as the reinforcement ratio increases, agreeing with the finding obtained by previous researchers [12 & 49]. The results obtained by the 4 x 5 x 1 ANN indicates that the trend of the punching shear strength is close to the cubic root of flexural reinforcement ratio, similar to the models provided by BS8110-97 and CEB-FIP-90 codes. However, when $\rho \geq 1.8\%$, the rate of increase of the punching shear strength with the increase of the reinforcement ratio is significantly reduced as depicted in Fig. 15.

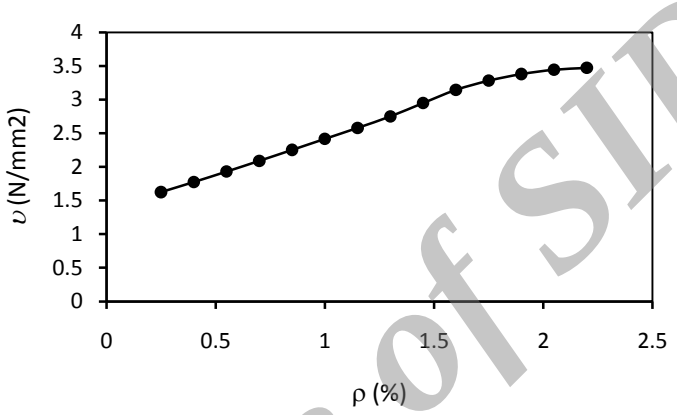

Figure 15 Reinforcement ratio, ρ effect on punching shear strength

5.4 Effect of perimeter of loaded area

The loaded section effect represented by the total perimeter of supported area, C, regardless of the loaded section shape on the punching shear strength is studied using the trained ANN. Previous researchers represented the loaded area differently by considering one side dimension of the loaded section, for example the width of loaded area [12 & 47]. However, currently there is no code takes into account the influence of the loaded section size in the punching shear strength calculation. Fig. 16 shows the effect of the total perimeter , C, of supported area on the punching shear strength of flat slabs. The punching shear strength decreases as the total perimeter of supported area increases, reasonably agreeing with the experimental results in the database. It, however, contradicts with the finding by Moe [12], where it was concluded that punching shear strength of flat slabs with side dimension greater than 0.75d increases as the width of loaded area increases. When the loaded area is very small, the flat slab is likely to fail in local crushing and the slab strength could not accurately predicted.

Archive of SID

www.SID.ir

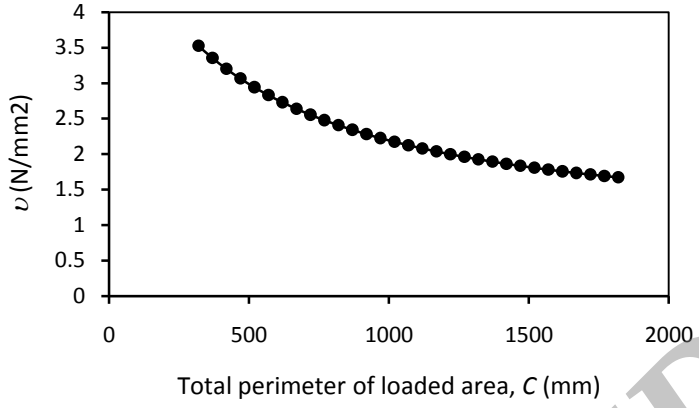

Figure 16. Perimeter of loaded area, *C*, effect on punching shear strength

6. PROPOSED DESIGN PUNCHING SHEAR STRENGTH EQUATION

The design assisted by testing approach proposed in Annex D of EN 1990 [18] is adopted to develop a simplified formula for the characteristic/design punching shear strength based on the trend predicted by the developed ANN as presented in Figs. 13 to 16 and the extensive experimental database collected in the current investigation. The mean value of the punching shear strength, v_m, is represented by the following probabilistic model, similar to the one proposed in BS8110-97:

$$v_m = b(100\rho)^{0.33}\left(\frac{400}{d}\right)^{0.25}\left(\frac{f_c'}{25}\right)^{0.33}\left(\frac{1}{100C}\right)^{0.5}\delta \text{ (N/mm}^2\text{)} \quad (5)$$

where b is a least-square fine-tuning parameter and δ is an error random variable, that may be obtained from a comparison of the experimental and predicted mean punching shear strengths for each specimen in the database; the values of b and δ can be given by the following equations:

$$b = \sum_{i=1}^{n}\left(v_{exp}\right)_i (v_m)_i \,/\, \sum_{i=1}^{n}(v_m)_i^2$$

$$\delta_i = \frac{(v_{exp})_i}{(bv_m)_i}$$

where n = 281. The least-square fine-tuning parameter b obtained from the 281 specimens collected is 1.4. The mean punching shear strength (v_m) can, then, be obtained by introducing the fine tuning parameter as below:

$$v_m = 1.4(100\rho)^{0.33}\left(\frac{400}{d}\right)^{0.25}\left(\frac{f_c'}{25}\right)^{0.33}\left(\frac{1}{100C}\right)^{0.5} \text{ (N/mm}^2\text{)} \quad (6)$$

Fig. 17 shows the comparison between the shear resistance obtained from Eq. 6 and the

Archive of SID

www.SID.ir

experimental results of all 281 test specimens. The mean value, Δ, standard deviation, σ, and coefficient of variation, *CoV*, of the error random variable δ can be given by the following equations:

$$\Delta = \frac{1}{n}\sum_{i=1}^{n}\delta_i$$

$$\sigma = \sqrt{\frac{1}{n-1}\sum_{i=1}^{n}(\delta_i - \Delta)^2}$$

$$\mathrm{CoV} = \sigma/\Delta$$

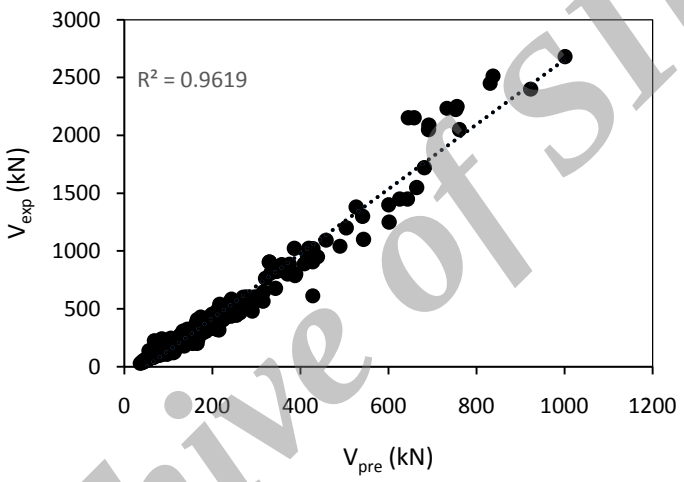

Figure 17. Comparisons between proposed model and 281 experimental results

Comparing the experimental results of the 281 test specimens with the predictions from the model presented in Eq. 6 produces: Δ= 1.016, σ = 0.255 and CoV = 0.251, indicating the high level of accuracy of the above model. These statistical values of δ are also particularly important for defining the 5th percentile of the punching shear strength from which the characteristic and design compressive strengths can be obtained.

The cumulative distribution of the error random variable δ compared against the theoretical Gaussian distribution having the same mean value and standard deviation is presented in Fig. 18. This comparison shows that the cumulative distribution of δ is close to the standard normal distribution curve, validating the normality hypothesis of error. Therefore, the characteristic value, v_k, of punching shear strength can be calculated from:

$$v_k = v_m - 1.64\sqrt{Var(v)}$$

The basic random variables, $f_c^{'}$, ρ, d and C can be considered as statistically independent variables, the variance, $Var(v)$, can, then, be calculated from equation (7) below:

Archive of SID

www.SID.ir

$$Var(v) = \sum [k_i^2 Var(x_i)] + k_\delta^2 Var(\delta) \quad (7)$$

The four variables considered in the punching shear strength (Eq. 6) can be divided into two categories; namely the geometrical parameters (ρ, d and C) and material properties ($f_c^{'}$). Assuming the parameters related to the slab geometry are deterministic variables with zero variation and concrete compressive strength $f_c^{'}$ is normally distributed random variable, the variation of v may be written as below:

$$Var(v) = \left(\frac{\partial v}{\partial f_c^{'}}\right)^2 Var\left(f_c^{'}\right) + \left(\frac{\partial v}{\partial \delta}\right)^2 Var(\delta) \quad (8)$$

where

$$\frac{\partial v}{\partial f_c^{'}} = 0.018(100\rho)^{0.33}\left(\frac{400}{d}\right)^{0.25}\left(\frac{f_c^{'}}{25}\right)^{-0.67}\left(\frac{1}{100C}\right)^{0.5}$$

$$\frac{\partial v}{\partial \delta} = 1.4(100\rho)^{0.33}\left(\frac{400}{d}\right)^{0.25}\left(\frac{f_c^{'}}{25}\right)^{0.33}\left(\frac{1}{100C}\right)^{0.5}$$

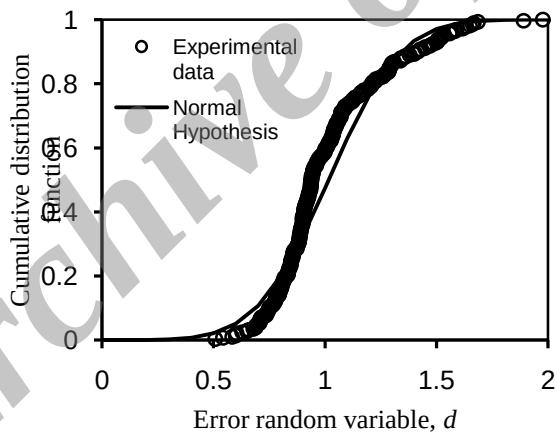

Figure 18. Cumulative frequency distribution of the model random variable, δ

As the number of specimens used in each experimental investigation collected from the literature were very small to allow the calculations of the coefficient of variations for $f_c^{'}$, a nominal value of CoV for $f_c^{'}$ may be reasonably assumed as (BS EN 1992-1-1:2004):

CoV for $f_c^{'}$ =4.88/$f_c^{'}$

However, the coefficient of variation of δ is obtained from the statistical distribution of the comparison between the theoretical and 281 experimental punching shear capacities as obtained above (CoV=0.251).

The critical punching shear failure plane for this equation is assumed to be at a distance 0.5d from the loaded face, similar to ACI 318-11 and CSA-A23.03-04.

Archive of SID

www.SID.ir

7. CONCLUSIONS

Based on this study, the following conclusions can be drawn:

- The shear strengths predicted by CSA-A23.03-04 and ACI 318-11 codes are generally larger than that obtained from BS8110-97 and CEB-FIP-90. However, as the critical perimeter in the latter codes are larger than that in the former, the punching shear capacity is expected to be closer.
- Comparisons between punching shear capacities predicted by the code equations and experimental results of 218 flat slab test specimens show that the CEB-FIP-90 prediction is the most conservative and scatter, while BS 8110-97 prediction exhibit the least mean square error to experimental results.
- The punching shear capacity of reinforced concrete flat slabs can be modelled with reasonable accuracy using a single hidden layer having a small number of neurons. This type of network reduced the possibility of over-fitting problems.
- ANN shows to be considerably accurate compared to the four design methods considering its lowest percentage of mean square error and more reliable and consistent predictions with its lower standard deviation.
- Parametric study showed that the slab effective depth, concrete compressive strength, flexure reinforcement ratio and column perimeter are significant parameters that primarily affect the punching shear behaviour of slab-column connections of flat slabs.

Despite being a simple equation, the new proposed equation including the main four significant parameters can predict the punching shear capacity with a reasonable accuracy compared with other available design codes.

APPENDIX A: DETAILS OF TEST SPECIMENS IN THE DATABASE

ID	Col. Section	L (mm)	h (mm)	d (mm)	b_s (mm)	C (mm)	f_c' (MPa)	ρ (%)	V_{exp} (kN)	V_{exp}/V_{code}				Ref.
										ACI 318	CEB-FIP	BS8110	CSA A23	
H1	S	3270	155	129	180	720	38	0.88	453	1.250	1.517	1.319	1.213	[19]
AR2	S	2300	100	80	200	800	39.1	1.64	258	1.247	1.500	1.128	1.212	[20]
AR9	S	2300	100	80	200	800	37.1	1.64	251	1.246	1.485	1.098	1.210	
DF1	S	2300	100	69	200	800	24.8	1.89	191	1.400	1.562	1.047	1.359	[21]
DF4	S	2300	120	88	200	800	19.8	1.2	199	1.197	1.380	0.999	1.161	
1D1	S	1800	120	87	200	800	39.8	1.2	269	1.163	1.511	1.169	1.123	[22]
PG11	S	3000	250	208	260	1040	31.5	0.77	763	1.058	1.222	1.127	0.919	
PG19	S	3000	250	208	260	1040	46.2	0.78	860	0.998	1.225	1.185	0.867	[23]
PG20	S	3000	250	208	260	1040	51.7	1.56	1094	1.243	1.237	1.243	1.080	
PG2-B	S	3000	250	210	260	1040	40.5	0.25	438	0.52	0.926	0.856	0.459	
PG5	S	3000	250	210	260	1040	29.3	0.33	550	0.72	1.179	1.085	0.677	[24]
PG3	S	6000	500	456	520	2080	32.4	0.33	2153	0.64	1.147	1.082	0.559	
ND651-1	S	3000	320	275	200	800	64.3	1.99	2050	1.483	1.282	1.430	1.291	[25]
P200	S	1450	240	200	200	800	39.5	0.83	904	1.362	1.473	1.375	1.183	[26]
Slab 1	S	2800	250	210	450	1800	36.5	1.07	968	0.87	1.112	0.992	0.761	[27]
Slab 2	S	2800	250	210	450	1800	41.9	1.07	950	0.80	1.042	0.945	0.697	
P01	C	2700	200	155	300	943	47.2	2.1	612	0.78	0.764	0.703	0.678	[28]
P02	C	2700	200	155	300	943	47.2	2.1	906	1.15	1.131	1.041	1.004	
BD1	S	1500	125	101	100	400	52.8	1.28	293	1.504	1.474	1.275	1.307	[29]
BD4	S	1500	125	101	100	400	46	1.28	293	1.612	1.543	1.275	1.400	

Archive of SID

www.SID.ir

ID	Col. Section	L (mm)	h (mm)	d (mm)	b_s (mm)	C (mm)	f_c' (MPa)	ρ (%)	V_{exp} (kN)	V_{exp}/V_{code}				Ref.
										ACI 318	CEB-FIP	BS8110	CSA A23	
A-1b	S	1828	152	118	254	1016	25.4	1.16	365	1.249	1.438	1.124	1.085	
A-1c	S	1828	152	118	254	1016	29	1.16	356	1.140	1.343	1.049	0.991	
A-1d	S	1828	152	118	254	1016	36.8	1.16	351	0.998	1.223	0.956	0.867	
A-1e	S	1828	152	118	254	1016	20.3	1.16	356	1.363	1.512	1.180	1.184	
A-2b	S	1828	152	118	254	1016	19.5	2.5	400	1.636	1.519	1.092	1.421	
A-2c	S	1828	152	118	254	1016	37.4	2.5	467	1.378	1.428	1.028	1.197	
A-7b	S	1828	152	118	254	1016	29.7	2.5	512	1.696	1.691	1.217	1.473	
A-3b	S	1828	152	118	254	1016	22.6	3.74	445	1.690	1.610	1.089	1.468	
A-4	S	1828	152	118	356	1424	26.1	1.18	400	1.060	1.362	1.039	0.921	[30]
A-5	S	1828	152	118	356	1424	27.8	2.5	534	1.431	1.577	1.107	1.244	
A-6	S	1828	152	118	356	1424	25	3.74	498	1.408	1.523	1.007	1.223	
A-13	S	1828	152	118	356	1424	26.2	0.55	236	0.605	0.995	0.764	0.526	
B-1	S	1828	152	118	254	1016	14.6	0.48	178	0.841	1.198	0.922	0.731	
B-2	S	1828	152	118	254	1016	47.6	0.48	200	0.523	0.908	0.743	0.455	
B-4	S	1828	152	118	254	1016	47.9	1.01	334	0.871	1.181	0.970	0.757	
B-9	S	1828	152	118	254	1016	43.9	2	505	1.376	1.464	1.171	1.195	
B-14	S	1828	152	118	254	1016	50.5	3.02	578	1.468	1.600	1.172	1.276	
5	S	1840	150	117	150	471	26.8	0.8	255	1.194	1.324	1.065	1.037	
6	S	1840	150	118	150	471	26.2	0.79	275	1.287	1.423	1.148	1.118	
24	S	1840	150	128	300	942	26.4	1.01	430	1.157	1.444	1.144	1.005	
25	S	1840	150	124	300	942	25.1	1.04	408	1.173	1.453	1.140	1.019	
32	S	1840	150	123	300	942	26.3	0.49	258	0.732	1.178	0.919	0.636	
33	S	1840	150	125	300	942	26.6	0.48	258	0.713	1.151	0.903	0.619	
IA 15a-5	S	1840	150	117	106	333	23.6	0.8	255	1.524	1.487	1.218	1.427	
IA 15a-6	S	1840	150	118	106	333	23	0.79	275	1.643	1.600	1.313	1.486	
IA 15c-11	S	1840	150	121	106	333	28.8	1.53	333	1.711	1.377	1.142	1.487	[15]
IA 15c-12	S	1840	150	122	106	333	27.7	1.54	331	1.713	1.363	1.133	1.349	
IA 30a-24	S	1840	150	128	212	666	23.2	1.01	430	1.554	1.691	1.371	1.377	
IA 30a-25	S	1840	150	124	212	666	21.9	1.04	408	1.585	1.709	1.372	1.563	
IA 30c-30	S	1840	150	120	212	666	26.8	2.16	490	1.799	1.632	1.267	1.739	
IA 30c-31	S	1840	150	119	212	666	26.8	2.18	539	2.002	1.821	1.406	0.857	
IA 30d-32	S	1840	150	123	212	666	23.1	0.49	258	0.986	1.383	1.105	0.833	
IA 30a-33	S	1840	150	125	212	666	23.4	0.48	258	0.959	1.349	1.083	1.111	
IA 30a-34	S	1840	150	120	212	666	24.2	1	331	1.279	1.437	1.142	1.145	
IA 30a-35	S	1840	150	122	212	666	21.8	0.98	331	1.318	1.456	1.163	1.035	
R-1	S	1828	152	114	305	1220	27.5	1.38	394	1.192	1.409	1.076	1.315	
R-2	S	1828	152	114	152	608	26.5	1.38	312	1.514	1.414	1.130	1.270	
S1-60	S	1828	152	114	254	1016	23.2	1.06	390	1.462	1.728	1.334	1.190	
S2-60	S	1828	152	114	254	1016	22	1.03	356	1.370	1.621	1.251	1.074	
S3-60	S	1828	152	114	254	1016	23.8	1.13	334	1.236	1.436	1.110	1.248	
S1-70	S	1828	152	114	254	1016	24.4	1.06	393	1.436	1.712	1.323	1.182	[12]
S2-70	S	1828	152	114	254	1016	25.3	1.02	379	1.361	1.652	1.276	0.990	
S4-70	S	1828	152	114	254	1016	35.1	1.13	374	1.139	1.413	1.093	1.083	
S4A-70	S	1828	152	114	254	1016	20.4	1.13	312	1.247	1.412	1.091	1.667	
S5-60	S	1828	152	114	203	812	22.1	1.06	343	1.529	1.664	1.304	1.328	
S5-70	S	1828	152	114	203	812	24.2	1.06	379	1.615	1.784	1.399	1.403	
M1A	S	1828	152	114	305	1220	23	1.5	433	1.4312	1.598	1.221	1.244	
I	S		102	82	221	694	13.9	1.21	182	1.488	1.645	1.153	1.293	
II-4a	S		102	82	221	694	23.8	0.89	245	1.531	2.051	1.439	1.329	
II-5	S		102	82	221	694	22.8	0.53	152	0.971	1.534	1.074	0.843	
II-6	S		102	82	221	694	12.3	1.33	157	1.365	1.432	1.004	1.185	
II-8	S		102	82	333	1046	24.8	0.59	219	0.978	1.722	1.172	0.850	[31]
IIR20-2	S		102	82	201	631	19.8	0.93	307	1.547	1.746	1.349	1.343	
III-3	S		102	82	221	694	24	1.21	201	1.251	1.515	1.064	1.086	
7	S		102	82	119	373	13.2	0.74	118	1.493	1.570	1.145	1.296	

Archive of SID

www.SID.ir

ID	Col. Section	L (mm)	h (mm)	d (mm)	b_s (mm)	C (mm)	f_c' (MPa)	ρ (%)	V_{exp} (kN)	V_{exp}/V_{code}				Ref.
										ACI 318	CEB-FIP	BS8110	CSA A23	
M3-1-0	S	610	70	51	152	608	21.1	1.1	79	1.258	1.591	0.984	1.093	
M3-1-0a	S	610	70	51	152	608	18	2.2	99	1.707	1.722	1.034	1.483	
M4-1-0M	S	813	70	51	203	812	15.5	1.1	93	1.381	1.815	1.099	1.200	
M4-2-0	S	813	70	50	203	812	27.2	2.2	133	1.527	1.817	1.063	1.326	
M5-1-0	S	1016	70	51	254	1016	23.3	1.1	109	1.099	1.650	0.985	1.016	
M5-2-0	S	1016	70	51	254	1016	22.9	2.2	152	1.547	1.897	1.099	1.429	
M6-1-0	S	12201	70	51	305	1220	23	1.1	114	0.992	1.560	0.919	0.982	
M6-2-0	S	220	70	50	305	1220	26.4	2.2	159	1.321	1.751	0.996	1.317	
M7-1-0	S	1422	70	51	356	1424	27.7	1.1	139	0.964	1.625	0.949	1.009	
M7-2-0	S	1422	70	51	356	1424	25	2.2	184	1.343	1.824	1.033	1.406	[32]
M8-1-0	S	1626	70	51	406	1624	24.9	1.1	145	0.944	1.612	0.933	1.033	
M8-2-0	S	1626	70	50	406	1624	24.6	2.2	185	1.239	1.738	0.970	1.365	
M3-1-2	S	610	70	50	152	608	27	1.1	102	1.472	1.952	1.201	1.279	
M2-1-0	S	406	70	50	102	408	28.5	1.1	86	1.606	1.884	1.192	1.395	
M2-2-0	S	406	70	50	102	408	24.9	2.2	102	2.037	1.915	1.176	1.770	
M3-1-0b	S	610	70	50	152	608	53.8	2.2	172	1.758	2.144	1.415	1.527	
M3-1-4a	S	610	70	50	152	608	21.1	1.1	99	1.616	2.056	1.264	1.404	
M3-1-4b	S	610	70	50	152	608	20	1.1	112	1.878	2.368	1.456	1.631	
M3-2-4	S	610	70	50	152	608	17	2.2	105	1.910	1.921	1.146	1.659	
1	C	1190	120	100	125	392	35.7	0.8	216	1.217	1.404	1.088	1.057	
3	C	1190	119	99	125	392	28.6	0.81	194	1.239	1.376	1.063	1.076	
5	C	2380	120	200	250	785	30.3	0.8	603	0.922	1.035	0.954	0.800	
6	C	2380	219	199	250	785	28.6	0.8	600	0.951	1.059	0.974	0.826	[33]
13	C	1190	118	98	125	392	33.3	0.35	145	0.871	1.316	1.011	0.756	
14	C	1190	119	99	125	392	31.4	0.34	148	0.902	1.358	1.047	0.784	
17	C	2380	220	200	250	785	31.7	0.34	489	0.731	1.099	1.010	0.635	
18	C	2380	217	197	250	785	30.2	0.35	444	0.695	1.031	0.944	0.604	
SS2	S	1830	100	77	200	800	23.3	1.2	176	1.295	1.546	1.071	1.125	
SS4	S	1830	100	77	200	800	33.4	0.92	194	1.192	1.651	1.145	1.035	
SS6	S	1830	100	79	200	800	21.7	0.75	165	1.217	1.665	1.162	1.057	
SS7	S	1830	100	79	200	800	31.2	0.8	186	1.144	1.628	1.137	0.994	
SS8	S	1830	250	200	250	1000	36.3	0.98	825	1.153	1.246	1.149	1.001	
SS9	S	1830	160	128	160	640	34.5	0.98	390	1.364	1.462	1.207	1.185	[34]
SS10	S	1830	160	128	160	640	35.7	0.98	365	1.255	1.353	1.117	1.090	
SS11	S	1830	80	64	80	320	34.5	0.98	117	1.637	1.755	1.218	1.422	
SS12	S	1830	80	64	80	320	35.7	0.98	105	1.444	1.557	1.080	1.254	
SS13	S	1830	80	64	80	320	37.8	0.98	105	1.404	1.528	1.060	1.219	
1	S	700	51	40.5	100	400	31.5	0.42	36	0.854	0.496	0.884	0.742	
2	S	700	51	40.5	100	400	31.5	0.56	49	1.162	1.850	1.094	1.009	
3	S	700	51	40.5	100	400	31.5	0.69	57	1.352	2.007	1.188	1.174	
4	S	700	51	40.5	100	400	36.2	0.82	56	1.239	1.777	1.053	1.076	
5	S	700	51	40.5	100	400	36.2	0.88	57	1.261	1.767	1.047	1.095	
6	S	700	51	40.5	100	400	36.2	1.03	66	1.460	1.942	1.151	1.268	
7	S	700	51	40.5	100	400	30.4	1.16	71	1.714	2.128	1.261	1.489	
8	S	700	51	40.5	100	400	30.4	1.29	71	1.714	2.054	1.218	1.489	
9	S	700	51	40.5	100	400	30.4	1.45	79	1.907	2.198	1.304	1.657	
10	S	700	51	40.5	100	400	30.6	0.52	44	1.058	1.718	1.016	0.919	[35]
11	S	700	51	40.5	100	400	30.6	0.8	55	1.324	1.861	1.102	1.149	
12	S	700	51	40.5	100	400	30.6	1.11	67	1.612	2.033	1.205	1.400	
13	S	700	51	40.5	100	400	35.3	0.6	49	1.098	1.740	1.030	0.953	
14	S	700	51	40.5	100	400	35.3	0.69	52	1.165	1.763	1.044	1.012	
15	S	700	51	40.5	100	400	35.3	1.99	85	1.904	2.025	1.203	1.654	
1A	S	700	57	46.5	100	400	29.4	0.44	45	0.922	1.503	0.928	0.802	
2A	S	700	57	46.5	100	400	29.4	0.69	66	1.354	1.897	1.173	1.176	
3A	S	700	57	46.5	100	400	29.4	1.29	90	1.846	2.100	1.301	1.603	
4A	S	700	57	46.5	100	400	31.7	1.99	97	1.916	1.911	1.186	1.664	

Archive of SID

www.SID.ir

ID	Col. Section	L (mm)	h (mm)	d (mm)	b_s (mm)	C (mm)	f_c' (MPa)	ρ (%)	V_{exp} (kN)	V_{exp}/V_{code}				Ref.
										ACI 318	CEB-FIP	BS8110	CSA A23	
1B	S	700	45.5	35	100	400	39.6	0.42	29	0.738	1.410	0.796	0.642	
2B	S	700	45.5	35	100	400	39.6	0.69	38	0.968	1.566	0.885	0.841	
3B	S	700	45.5	35	100	400	39.6	1.29	57	1.452	1.908	1.080	1.261	
4B	S	700	45.5	35	100	400	31.7	1.99	73	2.078	2.277	1.290	1.805	
1C	S	700	64	53.5	100	400	28.3	1.42	63	1.092	1.713	1.106	0.949	
2C	S	700	64	53.5	100	400	33.5	0.69	88	1.402	1.918	1.240	1.218	
3C	S	700	64	53.5	100	400	33.5	1.29	124	1.976	2.194	1.421	1.716	
4C	S	700	64	53.5	100	400	28.3	1.99	126	2.185	2.041	1.323	1.897	
S1.1	C	1190	120	100	125	392	28.6	0.8	216	1.360	1.511	1.171	1.181	
S1.2	C	1190	119	99	125	392	22.9	0.81	194	1.385	1.482	1.144	1.203	
S2.1	C	2380	220	200	250	785	24.2	0.8	603	1.032	1.115	1.027	1.896	
S2.2	C	2380	219	199	250	785	22.9	0.8	600	1.063	1.140	1.048	0.923	[36]
S1.3	C	1190	118	98	125	392	26.6	0.35	145	0.975	1.418	1.089	0.846	
S1.4	C	1190	119	99	125	392	25.1	0.34	148	1.009	1.464	1.127	0.876	
S2.3	C	2380	220	200	250	785	25.4	0.34	489	0.817	1.183	1.087	0.709	
S2.4	C	2380	217	197	250	785	24.2	0.35	444	0.776	1.110	1.015	0.674	
8	C	1117	101	76	102	320	24.1	2.05	129	1.472	1.198	0.858	1.278	
9	C	686	101	76	102	320	22.6	2.05	136	1.602	1.290	0.924	1.391	
10	C	381	101	76	102	320	24.6	2.05	129	1.457	1.190	0.853	1.265	
11	C	686	152	113	152	477	22.6	2.14	311	1.655	1.334	1.040	1.437	
12	C	686	152	113	203	638	24.8	2.14	357	1.521	1.369	1.049	1.321	
13	C	686	153	122	203	638	24.8	0.66	271	1.040	1.320	1.056	0.903	
14	C	533	102	73	152	477	25	5.01	202	1.863	1.764	1.074	1.618	
15	C	533	102	81	152	477	25	1.47	160	1.285	1.302	0.935	1.115	
16	C	533	102	86	152	477	23.2	0.45	107	0.822	1.196	0.872	0.714	[8]
17	C	533	102	81	102	320	25.5	1.47	121	1.225	1.093	0.804	1.063	
19	C	686	152	123	203	638	22.1	0.47	271	1.089	1.515	1.213	0.946	
20	C	686	152	113	203	638	15.1	2.14	278	1.518	1.258	0.962	1.318	
21	C	686	153	122	203	638	16.1	0.66	230	1.095	1.294	1.033	0.951	
23	C	533	102	81	152	477	14.5	1.47	108	1.138	1.053	0.755	0.989	
25	C	686	153	122	203	638	52.1	0.66	306	0.810	1.164	1.018	0.703	
26	C	686	102	73	203	638	52.1	5.01	323	1.683	1.982	1.292	1.461	
27	C	533	102	81	152	477	52.1	1.47	243	1.351	1.548	1.216	1.174	
28	C	533	102	86	152	477	52.1	0.45	148	0.759	1.264	1.008	0.659	
NS1	S	1700	120	95	150	600	42	1.47	320	1.607	1.677	1.290	1.396	
HS1	S	1700	120	95	150	600	67	0.47	178	0.708	1.168	1.045	0.629	
HS2	S	1700	120	95	150	600	70	0.84	249	0.969	1.327	1.207	0.879	
HS7	S	1700	120	95	150	600	74	1.19	356	1.347	1.658	1.539	1.258	
HS3	S	1700	120	95	150	600	69	1.47	356	1.395	1.582	1.435	1.258	
HS4	S	1700	120	90	150	600	66	2.37	418	1.805	1.866	1.552	1.591	
NS2	S	1700	150	120	150	600	30	0.94	396	1.691	1.795	1.456	1.468	
HS5	S	1700	150	125	150	600	68	0.64	365	0.975	1.332	1.306	0.873	
HS6	S	1700	150	120	150	600	70	0.94	489	1.367	1.671	1.636	1.241	[14]
HS8	S	1700	150	120	150	600	69	1.11	436	1.227	1.417	1.380	1.107	
HS9	S	1700	150	120	150	600	74	1.61	543	1.476	1.523	1.521	1.378	
HS10	S	1700	150	120	150	600	80	2.33	645	1.686	1.640	1.599	2.637	
HS11	S	1700	90	70	150	600	70	0.95	196	1.152	1.677	1.386	1.047	
HS12	S	1700	90	70	150	600	75	1.52	258	1.466	1.844	1.563	1.378	
HS13	S	1700	90	70	150	600	68	1.87	267	1.593	1.840	1.510	1.426	
HS14	S	1700	120	95	220	220	72	1.47	498	1.486	1.930	1.729	1.369	
HS15	S	1700	120	95	300	300	71	1.47	560	1.342	1.921	1.679	1.227	
65-1-1	S	2500	300	275	200	800	64	1.49	2050	1.486	1.413	1.573	1.291	
95-1-1	S	2500	300	275	200	800	84	1.49	2250	1.424	1.417	1.727	1.417	
115-1-1	S	2500	300	275	200	800	112	1.49	2450	1.343	1.402	1.880	1.542	
95-1-3	S	1190	300	275	200	800	90	2.55	2400	1.467	1.339	1.543	1.511	[25]
65-2-1	S	2200	225	200	150	600	70	1.75	1200	1.552	1.327	1.516	1.409	
95-2-1D	S	2200	225	200	150	600	88	1.75	1100	1.269	1.127	1.389	1.292	
95-2-1	S	2200	225	200	150	600	87	1.75	1300	1.508	1.337	1.642	1.527	
115-2-1	S	2200	225	200	150	600	119	1.75	1400	1.389	1.297	1.768	1.645	

Archive of SID

www.SID.ir

ID	Col. Section	L (mm)	h (mm)	d (mm)	b_s (mm)	C (mm)	f_c' (MPa)	ρ (%)	V_{exp} (kN)	V_{exp}/V_{code}				Ref.
										ACI 318	CEB-FIP	BS8110	CSA A23	
95-2-3	S	2200	225	200	150	600	90	2.62	1450	1.654	1.410	1.603	1.703	
95-2-3D	S	2200	225	200	150	600	80	2.62	1250	1.512	1.264	1.382	1.469	
95-2-3D	S	2200	225	200	150	600	98	2.62	1450	1.585	1.371	1.603	1.703	
115-2-3	S	2200	225	200	150	600	108	2.62	1550	1.614	1.419	1.714	1.821	
95-3-1	S	1100	113	88	100	400	85	1.84	330	1.639	1.607	1.564	1.640	
HSC0	C	2400	225	200	250	785	90	0.8	965	0.856	1.152	1.392	0.882	
HSC1	C	2400	225	200	250	785	91	0.8	1021	0.901	1.215	1.473	0.933	
HSC2	C	2400	225	194	250	785	86	0.82	889	0.843	1.128	1.329	0.849	
HSC4	C	2400	225	200	250	785	92	1.19	1041	0.914	1.081	1.318	0.951	[37]
HSC6	C	2400	225	201	250	785	109	0.6	960	0.768	1.175	1.512	0.871	
HSC9	C	2400	225	202	250	785	84	0.33	565	0.511	0.913	1.076	0.509	
N/HSC8	C	2400	225	198	250	785	95	0.8	944	0.827	1.127	1.382	0.875	
1	C		125	98	150	471	88.2	0.58	224	0.743	1.185	1.175	0.758	
2	C	1372	125	98	150	471	56.2	0.58	212	0.881	1.303	1.112	0.766	
3	C	13721	125	98	150	471	26.9	0.58	169	1.016	1.327	1.010	0.882	
4	C	37213	125	98	150	471	58.7	0.58	233	0.948	1.412	1.222	0.823	
6	C	72137	125	98	150	471	101.8	0.58	233	0.720	1.175	1.222	0.788	
12	C	21372	125	98	150	471	60.4	1.28	319	1.279	1.471	1.288	1.111	
13	C	13721	125	98	150	471	43.4	1.28	297	1.405	1.528	1.200	1.220	
14	C	37213	125	98	150	471	60.8	1.28	341	1.363	1.569	1.377	1.184	[38]
16	C	72137	125	98	150	471	98.4	1.28	362	1.138	1.418	1.462	1.225	
21	C	21372	125	98	150	471	41.9	1.28	286	1.377	1.489	1.155	1.196	
22	C	13721	125	98	150	471	84.2	1.28	405	1.376	1.672	1.636	1.370	
23	C	37213	125	100	150	471	56.2	0.87	341	1.378	1.768	1.520	1.197	
25	C	72137	125	100	150	471	32.9	1.27	244	1.289	1.333	1.024	1.119	
26	C	2	125	100	150	471	37.6	1.27	294	1.453	1.537	1.181	1.262	
27	C		125	102	150	471	33.7	1.03	227	1.152	1.275	0.985	1.001	
S1-U	S	2300	150	110	225	900	37.2	0.96	301	1.015	1.303	1.004	0.881	
S1-B	S	2300	150	110	225	900	37.2	1.92	317	1.069	1.089	0.842	0.928	
S2-U	S	2300	150	110	225	900	57.1	0.96	363	0.988	1.363	1.183	0.858	[39]
S2-B	S	2300	150	110	225	900	57.1	1.92	447	1.216	1.332	1.159	1.056	
S3-U	S	2300	150	110	225	900	67.1	0.96	443	1.112	1.576	1.443	0988	
S3-B	S	2300	150	110	225	900	67.1	1.92	485	1.217	1.370	1.257	1.082	
P100	S	925	135	100	200	800	39.4	0.98	330	1.328	1.697	1.280	1.153	
P150	S	1190	190	150	200	800	39.4	0.9	583	1.340	1.542	1.319	1.164	
P300	S	1975	345	300	200	800	39.4	0.76	1381	1.111	1.216	1.161	0.965	[26]
P400	S	1975	450	400	300	1200	39.4	0.76	2224	0.959	1.151	1.105	0.833	
P500	S	1975	550	500	300	1200	39.4	0.76	2681	0.809	0.959	0.939	0.702	
PG-1	S	3000	250	210	260	1040	27.6	1.5	1024	1.496	1.353	1.249	1.299	
PG-2	S	3000	250	210	260	1040	28.5	0.25	445	0.640	1.056	0.971	0.556	
PG-2b	S	3000	250	210	260	1040	40.5	0.25	439	0.529	0.927	0.856	0.459	
PG-3	S	3000	504	464	520	2080	32.4	0.33	2153	0.628	1.116	1.055	0.545	
PG-4	S	3000	250	210	260	1040	32.2	0.25	408	0.552	0.930	0.855	0.479	
PG-5	S	3000	250	210	260	1040	29.3	0.33	550	0.780	1.179	1.085	0.677	[40]
PG-6	S	1500	136	96	130	520	34.7	0.25	236	1.399	1.336	1.023	1.215	
PG-7	S	1500	140	100	130	520	34.7	0.75	243	1.359	1.613	1.248	1.180	
PG-8	S	1500	142	102	130	520	34.7	0.33	141	0.766	1.188	0.923	0.665	
PG-9	S	1500	142	102	130	520	34.7	0.25	118	0.641	1.091	0.846	0.557	
PG-10	S	3000	250	210	260	1040	28.5	0.33	540	0.776	1.169	1.075	0.674	
C1	S	1190	120	100	250	1000	24	0.8	270	1.193	1.617	1.198	1.036	
C2	S	1190	120	100	250	1000	24.4	0.8	250	1.095	1.489	1.104	0.951	[41]
D1	S	1190	145	125	150	600	27.2	0.64	265	1.120	1.312	1.077	0.972	
NSC1	S	1190	200	158	250	1000	35	2.17	678	1.347	1.231	1.030	1.169	
HSC1	S	11901	200	138	250	1000	68.5	2.48	788	1.347	1.441	1.323	1.210	
HSC2	S	19011	200	128	250	1000	70	2.68	801	1.499	1.650	1.453	1.361	[42]
HSC3	S	90119	200	158	250	1000	66.7	1.67	802	1.154	1.248	1.272	1.023	
HSC4	S	01190	200	158	250	1000	61.2	1.13	811	1.218	1.479	1.463	1.058	

Archive of SID

www.SID.ir

ID	Col. Section	L (mm)	h (mm)	d (mm)	b_s (mm)	C (mm)	f_c' (MPa)	ρ (%)	V_{exp} (kN)	V_{exp}/V_{code}				Ref.
										ACI 318	CEB-FIP	BS8110	CSA A23	
HSC5	S	11901	150	113	250	1000	70	1.88	480	1.060	1.241	1.157	0.962	
NSC2	S	190	200	163	250	1000	33	0.52	479	0.938	1.317	1.138	0.815	
NSC3	S		150	105	250	1000	34	0.4	228	0.795	1.416	1.064	0.690	
NS1	S	1190	150	105	250	1000	44.7	0.45	219	0.666	1.194	0.932	0.578	
NS2	S	1190	200	153	250	1000	50.2	0.55	491	0.851	1.285	1.175	0.739	
NS3	S	1190	250	183	250	1000	35	0.35	438	0.708	1.102	1.987	0.615	
HS1	S	1190	250	183	250	1000	70	0.35	574	0.656	1.147	1.237	0.596	
NS4	S	1190	300	218	250	1000	40	0.73	882	1.036	1.247	1.156	0.899	
HS2	S	1190	300	218	250	1000	64.7	0.73	1023	0.944	1.233	1.341	0.825	[43]
HS3	S	1190	300	220	250	1000	76	0.43	886	0.745	1.190	1.364	0.705	
HS4	S	1190	350	268	400	1600	75	1.13	1721	0.841	1.112	1.256	0.791	
HS6	S	1190	350	263	400	1600	65.4	1.44	2090	1.123	1.341	1.446	0.986	
NS4	S	1190	400	313	400	1600	40	1.57	2234	1.199	1.260	1.171	1.041	
HS7	S	1190	400	313	400	1600	60	1.57	2513	1.101	1.239	1.317	0.956	
PM-1	S	1500	125	102	130	520	36.6	0.25	176	0.930	1.597	1.239	0.808	
PM-2	S	1500	125	102	130	520	36.5	0.49	224	1.185	1.625	1.263	1.029	[44]
PM-3	S	1500	125	102	130	520	37.8	0.82	324	1.689	1.962	1.528	1.466	
PM-4	S	1500	125	102	130	520	36.8	1.41	295	1.558	1.504	1.173	1.353	
Slab 1	S	1200	80	60	120	480	38.51	0.5	225	2.545	4.055	2.685	2.210	
Slab 2	S	1200	80	60	120	480	37.42	1.0	242	2.776	3.495	2.319	2.411	
Slab 3	S	1200	80	60	120	480	28.19	1.5	143	1.889	1.981	1.315	1.640	
Slab 4	S	1200	60	49.5	120	480	38.24	0.5	138	2.017	3.422	2.131	1.751	
Slab 5	S	1200	60	49.5	120	480	36.6	1.0	147	2.203	2.945	1.838	1.913	
Slab 6	S	1200	60	49.5	120	480	41.95	1.5	130	1.819	2.174	1.381	1.580	
Slab 7	S	1200	80	60	120	480	32.45	1.0	182	2.237	2.749	1.823	1.942	
Slab 8	S	1200	60	49.5	120	480	41.3	0.5	133	1.872	3.218	2.026	1.626	[45]
Slab 9	S	1200	60	49.5	120	480	33.14	1.0	115	1.812	2.383	1.486	1.573	
Slab 10	S	1200	80	60	120	480	37.45	1.0	189	2.165	2.726	1.809	1.880	
Slab 11	S	1200	60	49.5	120	480	40.43	0.5	113	1.603	2.745	1.716	1.392	
Slab 12	S	1200	60	49.5	120	480	37.04	1.0	116	1.717	2.300	1.436	1.491	
Slab 13	S	1200	80	60	120	480	37.72	1.0	172	1.964	2.476	1.643	1.706	
Slab 14	S	1200	60	49.5	120	480	34.71	0.5	85	1.299	2.168	1.350	1.128	
Slab 15	S	1200	60	49.5	120	480	33.03	1.0	92	1.442	2.895	1.182	1.252	

Note: L = slab length, h = overall depth of flat slabs; d = effective depth of flat slabs; b_s = column side dimension; C = overall perimeter of column; f_c' = concrete compressive strength; S = square column; C = circular column

REFERENCES

1. Elshafey AA, Rizk E, Marzouk H, Haddara MR. Prediction of punching shear strength of two way slabs, *Engineering Structures*, **33**(2011) 1742-53.
2. Flood I, Kartam N. Neural networks in civil engineering I: Principles and Understanding, *Journal of Computing in Civil Engineering*, No. 2, **8**(1994) 131-48.
3. British Standards Association (BS 8110) (1997). Structural use of concrete. Use of concrete. Part 1: Code of Practice for Design and Construction, BSI, Milton Keynes.
4. Comité Euro–International Du Béton–Fédération de la Précontrainte (CEB–FIP). Model Code. Bulletin D'Information, Lausanne, Switzerland, Nos. 203-305, 1990.
5. European Committee for Standardization Eurocode 2 (CEN). Design of concrete structures-Part 1.1: general rules and rules for buildings. Brussels, Belgium, (2004) 225 p.
6. ACI (American Concrete Institute). Building code requirements for structural concrete,

Archive of SID

www.SID.ir

ACI 318-11, Farmington Hills, Michigan, 2011.
7. CSA (Canadian Standards Association). Design of concrete structures for buildings, CSA-A23.3-04, Rexdale, Ontario, Canada, 2004.
8. Gardner NJ. Relationship of the punching shear capacity of reinforced concrete slabs with concrete strength, *ACI Structural Journal*, No. 1, **87**(1990) 66-71.
9. Bazant ZP. Cao Z Size effect in punching shear failure of slabs, *ACI Structural Journal*, (1987) 44-53.
10. Guandalini S, Burdet OL, Muttoni A. Punching tests of slabs with low reinforcement ratios, *ACI Structural Journal*, No. 1, **106**(2009) 87-95.
11. Graf O. Tests of reinforced concrete slabs under concentrated loads applied near one support, (In German), Deutscher Ausschuss fiir Eisenbeton, Berlin, Heft 73, (1933) 2p.
12. Moe J. Shearing strength of reinforced concrete slabs and footings under concentrated loads, Development Department Bulletin D47, Portland Cement Association, Skokie, Ill., April, (1961) 130 p.
13. Marzouk HM**,** Hussein A. Punching shear analysis of reinforced high-strength concrete slab, *Canadian Journal of Civil Engineering*, No. 6, **18**(1991) 954-63.
14. Marzouk HM, Hussein A. Experimental investigation on the behavior of high strength concrete slabs, *ACI Structural Journal*, No. 6, **88**(1991) 701-13.
15. Kinnunen S, Nylander H. Punching of concrete slabs without shear reinforcement. Transactions No. 158. Royal Institute of Technology, Stockholm, Sweden, (1960) 112 p.
16. Baumann T, Rusch H. Tests studying the dowel action of flexural tensile reinforcement in reinforced concrete beam, Berlin, Deutscher AusschussM r StahlbetonH, eft 210, 1970.
17. Vintzeleou EN, Tassios TP. Mathematical models for dowel action under monotonic and cyclic conditions, *Magazine of Concrete Research*, No. 134, **38**(1986) 13-22.
18. BS EN 1992-1-1. Eurocode 2: Design of Concrete Structures, Brussel, Belgium, 2004.
19. Eder MA, Vollum RL, Elghazouli AY, Abdel-Fatteh T. Modelling and experimental assessment of punching shear in flat slabs with shearheads, *Engineering Structures*, **32**(2010) 3911-24.
20. Ramos A. Punching in prestressed concrete flat slabs, Ph.D thesis, Lisbon, Technical University of Lisbon, 2003.
21. Faria D, Lucio V, Ramos A. Strengthening of flat slabs with post-tensioning using anchorages by bonding, Engineering Structure, **33**(2011) 2025-43.
22. Inacio M, Ramos A, Faria D. Strengthening of flat slabs with transverse reinforcement by introduction of steel bolts using different anchorage approaches, *Engineering Structures*, **4**(2012) 63–77.
23. Guidotti R. Poinconnement des Planchers – dalles avec collones superposes fortement sollicitees. PhD thesis, Ecole Polytechnique Federale de Lausanne, Switzerland, 2010.
24. Guandalini S. Poinconnement Symetrique des dalles en Beton Arme, PhD thesis, Ecole Polytechnique de Lausanne, Switzerland, 2006.
25. Tomaszewicz A. Punching shear capacity of reinforced concrete slabs. High Strength Concrete SP2-Plates and Shells. Report 2.3. Report No. STF70A93082. SINTEF. Trondheim; Norway, **36**(1993) p.
26. Li KKL. Influence of size on punching shear strength of concrete slabs, Master thesis,

Archive of SID

www.SID.ir

McGill University, Montreal, Canada, (2000) 92p.
27. Caldentey AP, Lavaselli PP, Peiretti HC, Fernandez FA. Influence of stirrup detailing on punching shear strength of flat slabs, *Engineering Structures*, **49**(2013) 855-65.
28. Wörle P. Enhanced shear punching capacity by the use of post installed concrete screws, *Engineering Structures*, **60**(2014) 41-61.
29. Ramos AP, Lucio VJG, Regan PE. Punching of flat slabs with in-plane forces, *Engineering Structures*, **33**(2011) 894-902.
30. Elstner R, Hognestad E. Shearing strength of reinforced concrete slabs, *ACI Journal Proceeding*, No. 1, **53**(1956) 29-58.
31. Yitzhaki D. Punching strength of reinforced concrete slabs, *ACI Journal Proceeding*, No. 5, **63**(1966) 527-40.
32. Mowrer R, Vanderbilt M. Shear strength of lightweight aggregate reinforced concrete flat plates, *ACI Journal Proceeding*, No. 11, **64**(1967) 722–9.
33. Kinnunen S, Nylander H, Tolf P. Investigations on punching at the division of building statics and structural engineering, *Nordisk Betong*, Stockholm, **3**(1978) 25–7.
34. Regan P, Walker P, Zakaria K. Tests of reinforced concrete flat slabs, CIRIA Project No. RP 220, Polytechnic of Central London, 1979.
35. Rankin G, Long A. Predicting the punching strength of conventional slab–column specimens, *Proceedings of the Institution of Civil Engineers*, Part 1, **82**(1987) 327–46.
36. Tolf P. Plattjocklekens inverkan pøa betongplattors høallfasthet vid genomstansning Försök med cirkulära platter, Bulletin No. 146. Department of Structural Mechanics and Engineering. Royal Institute of Technology, Stockholm, (in Swedish with summary in English), (1988) 64 p.
37. Hallgren M. Punching shear capacity of reinforced high strength concrete slabs. Bulletin 23, Department of Structural Engineering, Royal Institute of Technology, Stockholm, (1996) 206 p.
38. Ramdane K. Punching shear of high performance concrete slabs, *In: Proceedings of the 4th International Symposium on Utilization of High Strength High Performance Concrete*, Paris, (1996) 1015-26.
39. Carla M. Ghannoum. Design of High Strength Concrete on the Performance of Slab-column Specimens, Master Thesis, McGrill University, 1998.
40. Guandalini S, Burdet OL, Muttoni A. Punching tests of slabs with low reinforcement ratios, *ACI Structural Journal*, No. 1, **106**(2009) 87-95.
41. Sundquist H, Kinnunen S. The effect of column head and drop panels on the punching capacity of flat slabs. Bulletin No. 82. Department of Civil and Architectural Engineering. Royal Institute of Technology. Stockholm, (in Swedish with summary and Figure captions in English), (2004) 24 p.
42. Marzouk H, Hossin M. Analysis of reinforced concrete two-way slabs. Research Report RCS01, Faculty of Engineering and Applied Science, Memorial University of Newfoundland, St. John's, Newfoundland, (2007)159 p.
43. Marzouk H, Rizk E. Punching analysis of reinforced concrete two-way slabs, Research Report RCS01, Faculty of Engineering and Applied Science, Memorial University of Newfoundland, St. John's, Newfoundland, Canada, (2009) 159 p.
44. Muttoni A. Tests on the Post-punching Behavior of Reinforced Concrete Flat slabs, Test

Archive of SID

www.SID.ir

Report, Ecole Polytechnique Federale de Lausanne Institut de Structures Laboratoire de Consruction en Beton, October 2008.
45. Jahangir Alam AKM, Amanat KM, Seraj SM. An experimental study on punching shear behaviour of concrete slabs, *Advances in Structural Engineering,* No. 2, **12**(2009) 257-65.
46. Bashir R, Ashour A. Neural network modelling for shear strength of concrete members reinforced with FRP bars, *Composites, Part B,* **43**(2012) 3198 -3207.
47. Regan PE. Symmetric punching of reinforced concrete slabs, *Magazine of Concrete Research*, No. 136, **38**(1986) 115-28.
48. Birkle G, Dilger WH. Influence of slab thickness on punching shear strength, *ACI Structural Journal*, No. 2, **105**(2008) 180-88.
49. Talbot AN. Reinforced Concrete Wall Footings and Column Footings, Bulletin No.67, University of IlIinois, *Engineering Experiment Station*, Urbana, **III**(1913) 114 p.

Archive of SID

www.SID.ir